0026-895X/90/040455-07$03.00/0
MOLECULAR PHARMACOLOGY, 38:455-461

Perturbations of Intracellular Calcium Distribution in Kidney Cells by Nephrotoxic Haloalkenyl Cysteine S-Conjugates

SPYRIDON VAMVAKAS, VIRENDRA K. SHARMA, SHEY-SHING SHEU, and M. W. ANDERS
Department of Pharmacology, University of Rochester, School of Medicine and Dentistry, Rochester, New York 14642
Received March 14, 1990; Accepted June 15, 1990

SUMMARY

The Ca^{2+}-sensitive dye fura-2 was used to investigate the disturbances in intracellular Ca^{2+} concentration ($[Ca^{2+}]_i$) and distribution induced by the nephrotoxic cysteine *S*-conjugate *S*-(1,2-dichlorovinyl)-L-cysteine (DCVC) and its homocysteine analog *S*-(1,2-dichlorovinyl)-L-homocysteine (DCVHC) in LLC-PK_1 cells. After 24-hr treatment with DCVC, the average $[Ca^{2+}]_i$ increased from 88 ± 23 nM to 415 ± 92 nM. Digital image analysis revealed that the mitochondrial region, which was stained with rhodamine-123, contained lower Ca^{2+} concentration ($[Ca^{2+}]$) than other cell areas. This distribution was different from the higher $[Ca^{2+}]$ in the nuclear and mitochondrial regions observed in control cells. In DCVHC-treated cells, there was also an increase in $[Ca^{2+}]_i$ to 355 ± 85 nM, but the increase in $[Ca^{2+}]$ was greater in the mitochondrial region, compared with the rest of the cell. After 72-hr treatment with DCVC or DCVHC, the average $[Ca^{2+}]_i$ was 410 ± 85 nM and 340 ± 90 nM, respectively, and blebs with markedly higher $[Ca^{2+}]$ (600–1000 nM) than the rest of the cell appeared in both DCVC- and DCVHC-treated cells. Moreover, in DCVC-treated cells the mitochondria could not be stained with rhodamine-123, indicating severe mitochondrial damage and loss of membrane potential. All changes described above took place in viable (propidium iodide-negative) cells. The experiments demonstrate that severe perturbations of intracellular Ca^{2+} distribution, particularly in the mitochondrial region, precede bleb formation and cell death in the course of development of toxocity by DCVC and DCVHC.

The nephrotoxicity and nephrocarcinogenity of trichloroethylene may be attributed to hepatic conjugation with glutathione to give *S*-(1,2-dichlorovinyl)-glutathione, processing of the glutathione conjugate to the corresponding cysteine conjugate DCVC, and renal metabolism of DCVC to reactive intermediates by cysteine conjugate β-lyase (1). DCVC is nephrotoxic *in vivo* (2) and is cytotoxic to freshly isolated renal cells (3) and to renal cells in culture (4). Although several coincidental changes occur during DCVC-induced cell injury, perturbations in mitochondrial energy status and Ca^{2+} homeostasis may play a central role in the sequence of events leading to cell death (3). In addition, DCVC is mutagenic in bacteria, induces DNA repair in LLC-PK_1 cells (a cultured cell line of porcine kidney), and causes DNA strand breaks in kidney tubules (5–8).

The role of Ca^{2+} in acute cell injury has been extensively studied (9, 10), but the range of events that take place during cell damage makes it difficult to distinguish causal effects from events that parallel cell death. One major limitation in the previous studies is the lack of information about the disturbances of $[Ca^{2+}]_i$ distribution in the intact living cells during the development of cell injury. Moreover, there are few studies on the role of Ca^{2+} as a link between acute cell injury and long term perturbations in cellular homeostasis. DCVC, which is cytotoxic, promotes the formation of *N,N*-dimethylnitrosamine-initiated tumors (11); DCVC metabolites also react with DNA (12). Hence, DCVC may find utility in the exploration of the role of Ca^{2+} in both short and long term toxicological processes. In the experiments described below, we investigated the temporal and spatial changes in $[Ca^{2+}]_i$ induced by DCVC and by its homocysteine analog DCVHC in LLC-PK_1 cells, which are sensitive to both the cytotoxic and genotoxic properties of cysteine *S*-conjugates (4, 7). FDIM was utilized to investigate microenvironmental changes in $[Ca^{2+}]_i$ that precede cell death during the development of toxicity in single living cells.

This research was supported by National Institute of Environmental Health Sciences Grant ES03127 (M.W.A.), National Institutes of Health Grant HL-33333, and American Heart Association-Established Investigatorship Award (S.-S.S.), American Heart Association/New York State Affiliate Grant-in-aid (V.K.S.), and Boehringer-Ingelheim (S.V.).

Materials and Methods

Chemicals. DCVC and DCVHC were obtained by synthesis (13, 14). All other chemicals were obtained from commercial sources.

ABBREVIATIONS: DCVC, *S*-(1,2-dichlorovinyl)-L-cysteine; $[Ca^{2+}]_i$ intracellular Ca^{2+} concentration; DCVHC, *S*-(1,2-dichlorovinyl)-L-homocysteine; FBS, fetal bovine serum; fura-2/AM, acetylmethyl ester of fura-2; CCCP, carbonyl-cyanide *m*-chlorophenylhydratone; $[Ca^{2+}]$, Free Ca^{2+} concentration; DMEM, Dulbecco's modified Eagle's medium; FDIM, fluorescence digital imaging microscopy; K_d, dissociation constant; HEPES, 4-(2-hydroxyethyl)-1-peperazineethanesulfonic acid; EGTA, ethylene glycol bis(β-aminoethyl ether)-*N,N,N',N'*-tetraacetic acid.

Cells and growth medium. LLC-PK$_1$ cells (passage 192–212; American Type Culture Collection) were grown in DMEM supplemented with 10% FBS, 3 g/liter glucose, 1.7 g/liter $NaHCO_3$, and 2 mM glutamine.

Cells (5×10^4) were plated in triplicate on sterilized, collagen-coated, cover glasses (25-mm diameter; VWR, San Francisco, CA) in 35-mm tissue culture dishes. After 10 hr, the medium was replaced with DMEM containing 2% FBS and the test compounds in the concentrations indicated in Results. In some experiments, the β-lyase inhibitor aminooxyacetic acid (Sigma, St. Louis, MO) or the amino group acceptor α-keto-γ-methiolbutyrate was added to the incubation medium at a concentration of 0.5 or 5 mM, respectively. The cells were incubated for 24, 48, 72, or 96 hr. Two hours before the end of the treatment period, hydroxyurea (10 mM) was added to some of the culture dishes, as indicated in Results, and was present when the cells were loaded with fura-2/AM (Molecular Probes, Eugene, OR).

Cell loading with fura-2/AM. Loading of LLC-PK$_1$ cells with fura-2/AM was difficult because this cell line is apparently able to secrete the free acid form of the dye. Sufficiently high intracellular concentrations of fura-2 could be obtained when the cells were loaded according to a modification of the method described by Poenie *et al.* (15). Cells were incubated with 2.5 mM probenecid for 30 min at 37° in DMEM containing 2% FBS and were washed twice with Hanks' buffer. Loading of the cells with fura-2/AM was performed in 2 ml of modified DMEM, which lacked sodium bicarbonate and FBS but contained 15 mM HEPES, 2.5 mM probenecid, and 2 μl of 10 mM fura-2/AM mixed with 1 μl of 25% pluronic acid and 27 μl of FBS; the final concentration of fura-2/AM in the incubation medium was 10 μM. Cells were incubated for 1 hr on an orbital shaker (90 rpm) at room temperature, washed once with Hanks' buffer, and then allowed to stand for 1 hr at room temperature in Hanks' buffer. In some of the experiments, 20 μl of rhodamine-123 (1 mg/ml of water; Eastman Kodak, Rochester, NY) were added per 2 ml of Hanks' buffer 30 min before the end of the 2-hr loading period, to stain the mitochondria.

FDIM. The use of FDIM in the present study has been described previously (16, 17). Briefly, after fura-2 loading, the cells were washed three times with HEPES buffer A, which contained 145 mM NaCl, 5 mM KCl, 2 mM $CaCl_2$, 10 mM glucose, and 10 mM HEPES (adjusted to pH 7.4 with 1 N NaOH). In some experiments, propidium iodide (50 nM), which selectively stains the nuclei of nonviable cells, was added in the HEPES buffer. The cover glasses were then removed from the culture dish and mounted in a tissue chamber. The cells were covered with a thin layer of HEPES buffer A, and the imaging was performed at room temperature on the stage of a Nikon inverted microscope equipped for epifluorescence with a 100× oil-immersion microscope objective (Nikon, Tokyo, Japan). At the beginning of each experiment, a camera (SIT camera; Dage MTI 65, Michigan City, IN) gain setting was found at which an optimal fluorescence intensity from loaded LLC-PK$_1$ cells was obtained. This setting was below the level at which autofluorescence from unloaded cells or background fluorescence from noncellular regions was detected, precluded the possibility of signal saturation (16), and was used throughout the experiment. The same gain setting was used for the calibration and determination of [Ca^{2+}] (see below). For every data point described in Results, at least four plates were studied and the fura-2 fluorescence of approximately 10 to 15 cells/plate was monitored.

First, a bright-field image of a cell or cell group was recorded for later comparison with the fluorescent images. The cell was then irradiated sequentially at 340 and 380 nm by manual insertion of a filter holder containing narrow bandpass filters (5- to 10-nm half-bandwidth; Omega Optical, Brattleboro, VT). To avoid phototoxicity and photobleaching, cells were exposed to the excitation light for 150 msec by the opening of an electronic shutter (Uniblitz; Vincent Associates, Rochester, NY). The emitted fluorescence images were acquired at 510 nm with a dichroic mirror (Omega Optical, Brattleboro, VT) focused onto the SIT camera. An image processor (FG-100-AT; Imaging Technology, Inc., Woburn, MA) housed in a microcomputer (Dell 286) was used to digitize the fluorescence images at a pixel resolution of 512

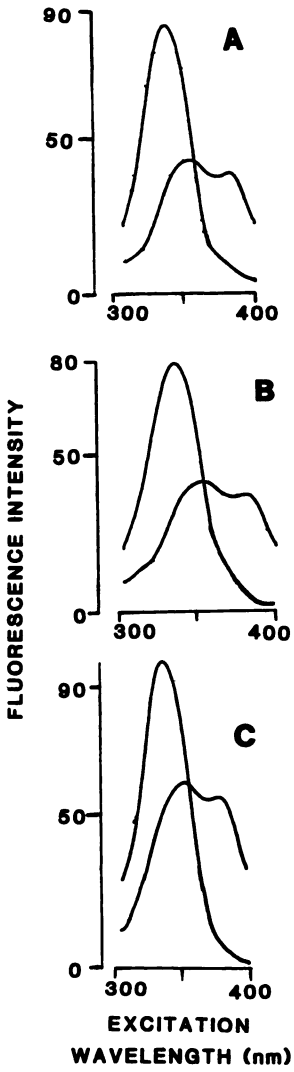

Fig. 1. Excitation spectra of cytosolic (A), mitochondrial (B), and free (C) Fura-2. The free Ca^{2+} concentration was either <1 nM or >100 μM. The pH of the solution was maintained at 7.2. One experiment, typical of three performed, is shown.

horizontal by 480 vertical. The fluorescence ratio image was obtained by dividing the 340-nm image by the 380-nm image on a pixel-by-pixel basis. Acquisition of a ratio image took about 2 to 4 sec. Excitation and emission wavelengths for rhodamine-123 were 546 and 580 nm, respectively. The H^+ ionophore CCCP, which dissipates the electrochemical gradient of mitochondria, was added to some plates at a concentration of 200 nM, and its effects on both the rhodamine staining and the fura-2 images were monitored over 30 min. Propidium iodide fluorescence was monitored at 490 nm.

Determination of the K_d and excitation spectra of fura-2 from cytosolic and mitochondrial fractions. After the cells were loaded with fura-2/AM, as described above, the cells were trypsinized and washed twice with HEPES buffer B, which contained 140 mM KCl, 10 mM NaCl, 1 mM K_2EGTA, 1 mM $MgCl_2$, and 10 mM HEPES (adjusted to pH 7.2); this buffer was used throughout the procedure, the cells were lysed with 4 μM digitonin (final concentration), and the cytosolic and mitochondrial cell fractions were obtained by sequential centrifugation at 1,000, 10,000, and 100,000 × *g*. The mitochondrial fraction was washed once at 10,000 × *g*, and the resulting pellet was treated with 0.1% Triton X-100 to release the dye.

Dissociation constants and excitation spectra of fura-2 from cytosolic and mitochondrial fractions and of fura-2 pentapotassium salt were determined at room temperature with a Perkin-Elmer LS-5 spectrofluorimeter. $CaCl_2$ was added to the cuvette to give [Ca^{2+}] ranging from

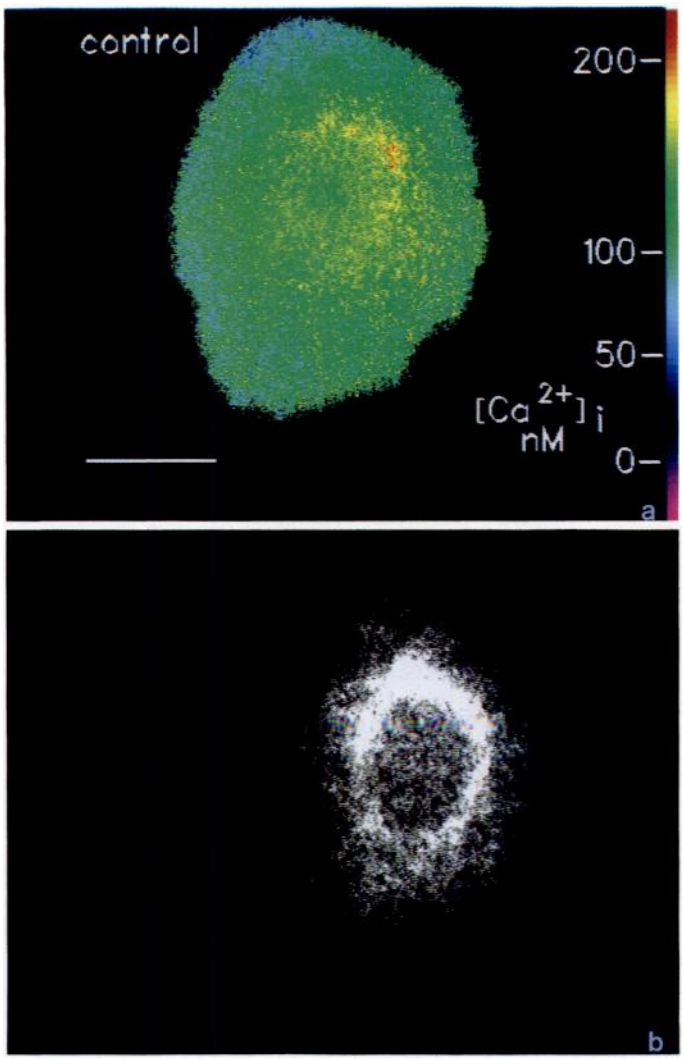

Fig. 2. Pseudocolor fluorescence ratio image (340 nm/380 nm) (A) and mitochondrial staining with rhodamine-123 (B) of a cell arrested in its growth by serum depletion and hydroxyurea treatment (for exact cell culture conditions, see Materials and Methods). The rainbow color spectrum correlates with the concentration of free Ca^{2+}, as calculated from *in vitro* calibration. The average $[Ca^{2+}]_i$ was 120 nM (*bar* = 3 μm).

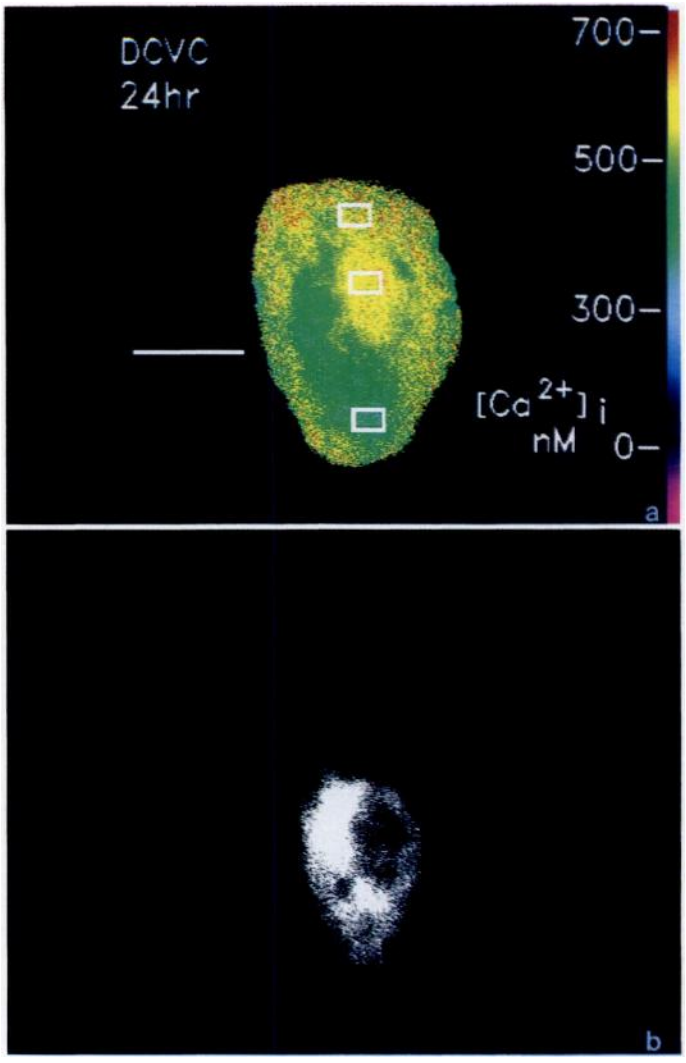

Fig. 3. Pseudocolor fluorescence ratio image (340 nm/380 nm) (A) and mitochondrial staining with rhodamine-123 (B) of a cell exposed for 24 hr to 10^{-4} M DCVC. The average $[Ca^{2+}]_i$ was 498 nM; $[Ca^{2+}]$ calculated from the mitochondria area (*lower rectangle*) was 380 nM, whereas nonmitochondria areas (*upper two rectangles*) showed $[Ca^{2+}]$ of approximately 570 and 600 nM, respectively (*bar* = 3 μm).

1 nM to >100 μM. The pH of the solution was carefully adjusted to 7.2 after each addition of $CaCl_2$. The amounts of $CaCl_2$ needed to give a certain $[Ca^{2+}]$ were calculated from the computer program developed by Fabiato (18).

Determination of $[Ca^{2+}]_i$. Based on the K_d for fura-2, which was determined as described above, only two HEPES buffer B solutions ($[Ca^{2+}]$-free and saturating $[Ca^{2+}]$) were needed to determine the entire calibration curve (19). The quantification of $[Ca^{2+}]_i$ can be obtained from the following equation:

$$[Ca^{2+}] = K_d \times \frac{(R - R_{min})}{(R_{max} - R)} \times \frac{Sf_2}{Sb_2}$$

where R is the measured cellular ratio and R_{min} and R_{max} are the ratios obtained in $[Ca^{2+}]_i$-free and saturating $[Ca^{2+}]$. Sf_2 is the 380-nm excitation signal in the absence of Ca^{2+}, and Sb_2 is the 380-nm excitation signal at saturating $[Ca^{2+}]$ in HEPES buffer B containing 3 μM fura-2 pentapotassium salt.

Results

Controls. Unless otherwise specified, the experiments were performed in cells whose growth was arrested by reduction of the FBS concentration from 10% to 2% and by addition of 10 mM hydroxyurea; these conditions reduce replicative DNA synthesis by approximately 95% without exerting cytotoxicity or influencing the effects of the *S*-conjugates (20). This treatment regimen prevented the monolayer from becoming confluent during the experiment (96 hr), allowed better focusing on individual cells and the generation of clearer Ca^{2+} distribution images, and removed the growth-dependent effects of $[Ca^{2+}]_i$.

In the absence of probenecid and at a loading temperature of 37°, fura-2 fluorescence revealed a spotty intracellular distribution of Ca^{2+}, with high concentrations in those areas of the cell rich in mitochondria, as shown by rhodamine-123 staining. Also, the overall intensity of the fluorescence signal decreased by approximately 50% over the first 60 min after the end of the loading time. In contrast, when the loading was performed at room temperature in the presence of 2.5 mM probenecid, the accumulation of the dye within discrete spots was reduced and dye leakage was less than 10% over the first hour after incubation. In the absence of the cysteine *S*-conjugates, probenecid was not toxic to the cells, as measured in preliminary experiments by lactate dehydrogenase leakage into the medium, and did not influence the Ca^{2+} distribution and concentration in LLC-PK_1 cells (data not shown).

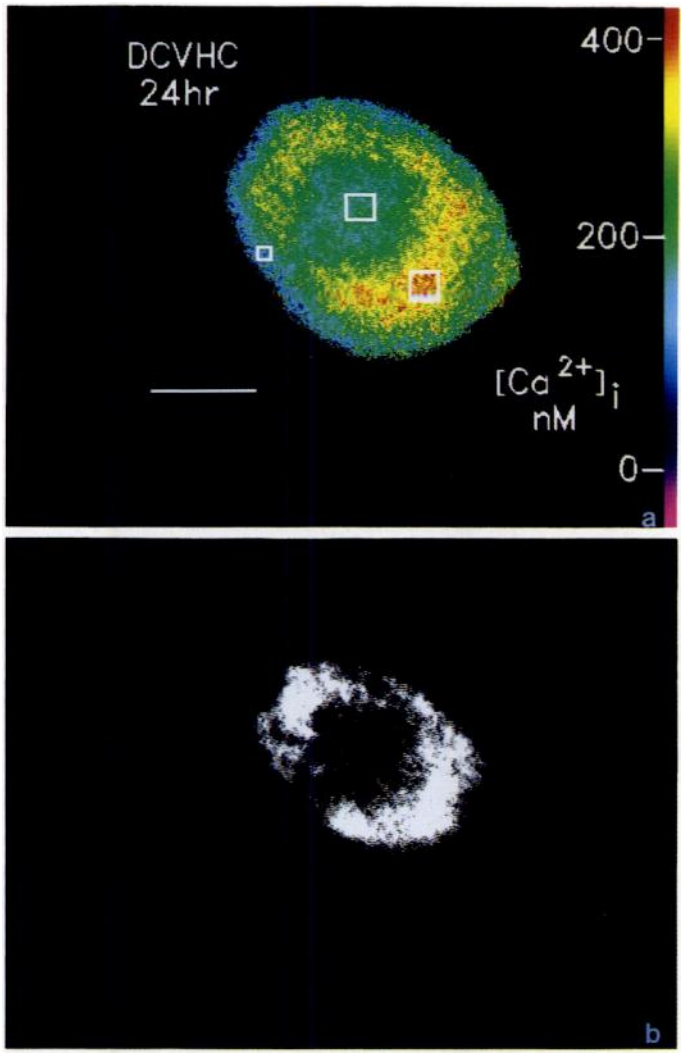

Fig. 4. Pseudocolor fluorescence ratio image (340 nm/380 nm) (A) and mitochondrial staining with rhodamine-123 (B) of a cell exposed for 24 hr to 10^{-4} M DCVHC. The average $[Ca^{2+}]_i$ was 280 nM; $[Ca^{2+}]$ from the mitochondrial area (*rectangle at the lower right side of the cell*) was approximately 400 nM, whereas the $[Ca^{2+}]$ calculated from the two other *rectangles*, placed over the nuclear and peripheral cytosolic parts of the cell, were 220 and 170 nM, respectively (*bar* = 3 μm).

The excitation spectra of fura-2 free acid and the dye samples obtained from cytosol and mitochondria were similar (Fig. 1). Also, the K_d values for Ca^{2+} from these three sources were the same [203 ± 21 nM, 206 ± 25 nM, and 208 ± 24 nM, respectively (n = 3)].

After inhibition of the replicative DNA synthesis, $[Ca^{2+}]$ was approximately 1.5 to 2.5 times higher in the nuclear and perinuclear regions, compared with the rest of the cell (Fig. 2A). The perinuclear region contains a high density of mitochondria, as indicated by the fluorescent image from rhodamine-123 (Fig. 2B). Cells grown in DMEM containing 10% FBS and not treated with hydroxyurea showed diverse Ca^{2+} distributions ranging from a diffuse pattern to high $[Ca^{2+}]$ in the nucleus or in mitochondria-rich areas of the cell. The average $[Ca^{2+}]_i$ in control cells was 85 ± 25 nM (n = 50) and 88 ± 29 nM for growing and growth-arrested cells, respectively. The Ca^{2+} ionophore A23187 (2 μM) increased the average $[Ca^{2+}]_i$ in control cells to 956 ± 65 nM (n = 5), indicating that the fura-2 inside the cell was Ca^{2+} sensitive. Addition of CCCP (200 nM) to the incubation solution for 30 min diminished the intensity of the rhodamine-123 staining by more than 70% and the fura-2 fluorescence ratio intensity in the rhodamine-123 staining areas by more than 50%. This indicates that the origin of the fura-2 fluorescence in the rhodamine-123-staining areas is mostly from mitochondrial Ca^{2+}.

DCVC-induced changes in Ca^{2+} homeostasis. The toxicity of DCVC was studied over 96 hr. Twenty-four hours after exposure of cells to 10^{-4} M DCVC, $[Ca^{2+}]_i$ increased from 88 ± 23 nM to 415 ± 92 nM (n = 50). Distinct areas of comparatively low $[Ca^{2+}]$ in the ratio image were observed in cells with elevated average $[Ca^{2+}]_i$. These areas of low $[Ca^{2+}]$ coincided with cellular areas rich in mitochondria, as shown by simultaneous rhodamine-123 staining. No changes in the rhodamine-123 pattern or intensity were observed, compared with untreated cells. The cell shown in Fig. 3A is a representative example; the average $[Ca^{2+}]_i$ was 498 nM, whereas the average $[Ca^{2+}]$ calculated from areas rich in mitochondria, as shown by rhodamine-123 staining (Fig. 3B), was about 380 nM. In contrast, extramitochondrial areas showed $[Ca^{2+}]$ between 570 and 600 nM. Blebs with lower $[Ca^{2+}]$ compared with the surrounding cytoplasm were observed in less than 10% of the cells after 24-hr exposure to DCVC. A similar pattern was obtained after 48-hr treatment. On the third day of exposure, the blebs became larger, were present in approximately 70% of the cells studied, and contained higher $[Ca^{2+}]$ than the rest of the cell. The average $[Ca^{2+}]_i$ was 410 ± 85 nM (n = 50), whereas values between 600 and 1000 nM were present in the blebs. Also, the rhodamine-123 pattern became more diffuse and less intense, and in about 50% of the cells the mitochondria could not be stained with rhodamine-123 after 72-hr treatment with DCVC. Ninety-six hours after treatment, most of the cells showed a diffuse Ca^{2+} distribution, the blebs increased in both number and size and could be identified as areas of high $[Ca^{2+}]$ in the ratio image. Rhodamine-123 staining was not observed in more than 90% of the cells.

DCVHC-induced changed in Ca^{2+} homeostasis. After 24-hr treatment with 10^{-4} M DCVHC in the presence of 5 mM α-keto-γ-methiolbutyrate, which enhances the toxicity of DCVHC (14), the $[Ca^{2+}]_i$ increased from 88 ± 23 nM to 355 ± 85 nM and exhibited a marked compartmentation; the mitochondria-rich areas showed $[Ca^{2+}]$ that was approximately 2 to 3 times higher than that in the surrounding cytosolic or the nuclear areas. No changes in the rhodamine-123 pattern or intensity were observed, compared with untreated cells. Fig. 4 shows the typical $[Ca^{2+}]_i$ of a cell exposed for 24 hr to DCVHC. The average $[Ca^{2+}]_i$ was 280 nM, whereas mitochondria-rich areas contained approximately 400 nM Ca^{2+}. In contrast, extramitochondrial areas contained 170 to 220 nM Ca^{2+}. On the first day of exposure to DCVHC, blebs were present in less than 10% of the cells, and these blebs contained no mitochondria and had lower $[Ca^{2+}]$ than the surrounding cytoplasm. This pattern did not change qualitatively on the second day of exposure to DCVHC. After 72 hr, areas of high $[Ca^{2+}]$ (600–1000 nM), which coincided with large blebs in the bright-field image, were detected in about 95% of the cells (Fig. 5). The average $[Ca^{2+}]_i$ was 340 ± 90 nM (n = 50). Rhodamine-123 staining did not show any differences, compared with untreated cells, although the high $[Ca^{2+}]$ observed in these organelles after 24 and 48 hr of treatment was less marked on the third day. This pattern was maintained after 96 hr of treatment; the only qualitative difference was observed in the rhodamine-123 staining of the mitochondria, which became less well defined and less intense, compared with controls and with earlier stages of toxicity. The mitochondria could, however, be stained in all cells treated with DCVHC for 96 hr; this result was different than the effects induced by DCVC. Finally, the β-lyase inhibitor

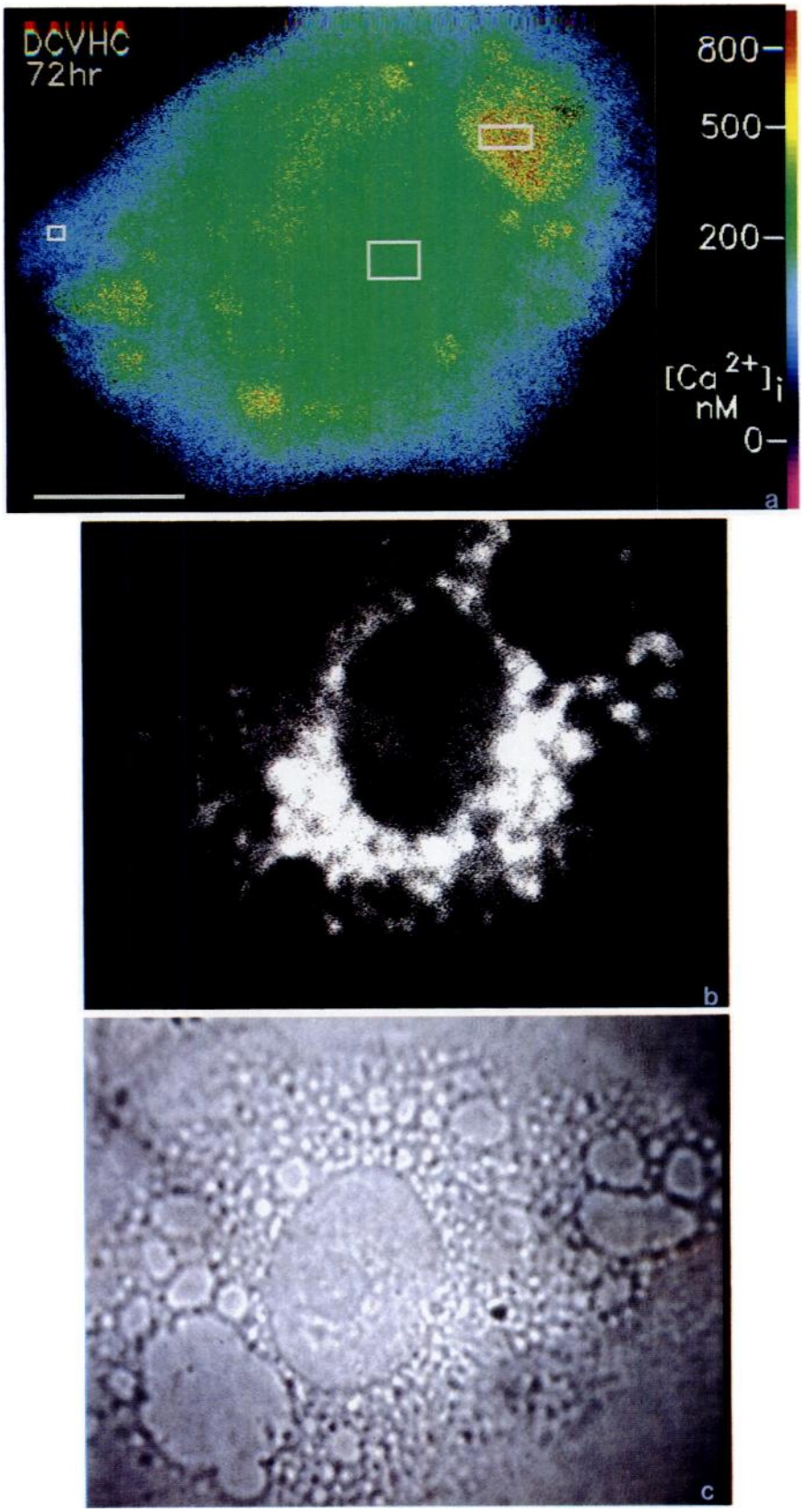

Fig. 5. Pseudocolor fluorescence ratio image (340 nm/380 nm) (A), mitochondrial staining with rhodamine-123 (B), and the bright field image (C) of a cell exposed for 72 hr to 10^{-4} M DCVHC. The average $[Ca^{2+}]_i$ was approximately 210 nM;$[Ca^{2+}]$ calculated from a bleb (*upper right rectangle*) was approximately 710 nM, whereas the two other *rectangles from areas lacking blebs contained* $[Ca^{2+}]$ *of 85 nM* (*rectangle at the far left of the cell*) and 280 nM (*rectangle over the nuclear area of the cell*) (*bar* = 3 μm).

aminooxyacetic acid (0.5 mM) prevented the changes in Ca^{2+} distribution and concentration induced by both DCVC and DCVHC.

For comparison, most studies were also performed in cells in exponential growth maintained in medium containing 10% FBS and no hydroxyurea. The absence of hydroxyurea did not alter the effects of DCVC or DCVHC on the Ca^{2+} distribution and concentration.

After 24-hr treatment with DCVC or DCVHC, approximately 10% of the cells stained positive with propidium iodide. The proportion of dead cells increased to approximately 20% after 96-hr exposure to the *S*-conjugate. However, all cells that

accumulated sufficient amounts of fura-2 to be studied with FDIM were viable according to propidium iodide staining.

Discussion

Loading of LLC-PK$_1$ cells with fura-2/AM at 37° in the absence of the anion transport inhibitor probenecid resulted in a marked accumulation of the dye in discrete spots in the mitochondria-rich perinuclear areas. In addition, under these loading conditions, the leakage of fura-2 into the medium within 1 hr following the loading procedure impaired the experiments, because the intracellular dye concentration became too low to allow studies of the spatial distribution of Ca^{2+}. Both the spotty labeling pattern of the cells and the dye leakage were reduced by loading of the cells with fura-2 at room temperature in the presence of 2.5 mM probenecid, which is consistent with previous reports (21, 22). There are several reports of the presence of Ca^{2+}-insensitive, but highly fluorescent, forms of fura-2 in cells that may result from incomplete deesterification of fura-2/AM (23). To investigate the spectral characteristics of fura-2 formed in cytosolic and mitochondrial fractions of control and treated LLC-PK$_1$ cells, spectrofluorimetric studies were performed with sequential addition of digitonin and Triton X-100 under Ca^{2+}-free and Ca^{2+}-saturating conditions. These experiments did not show any differences in either the excitation spectra or the K_d, compared with the results obtained with the free acid form of fura-2, indicating the presence of only two intracellular fluorescent forms of fura-2. The apparent absence of fluorescent, Ca^{2+}-insensitive, partially deesterified forms of fura-2/AM, in combination with the low leakage of the fluorescent probe from the cells, indicates that reliable values of $[Ca^{2+}]_i$ can be obtained with the calibration method described above.

The main objective of these experiments was to study spatial and temporal changes in the intracellular distribution of Ca^{2+} caused by two *S*-conjugates, rather than to quantify precisely the $[Ca^{2+}]_i$. Intracellular Ca^{2+} distribution varies among the different phases of the cell cycle (24). Subconfluent monolayers incubated with DMEM containing 10% FBS, which consist of cells in different growth phases, showed intracellular Ca^{2+} distributions ranging from a diffuse pattern to high $[Ca^{2+}]$ in the nucleus or in mitochondria-rich areas of the cell; the control values for $[Ca^{2+}]_i$ were similar to previously reported concentrations for LLC-PK$_1$ cells (25–27). Treatment of LLC-PK$_1$ monolayers with hydroxyurea, which blocks the conversion of ribonucleotides to deoxyribonucleotides, and serum deprivation diminish replicative DNA synthesis (20). This treatment results in a consistent distribution of intracellular Ca^{2+} among the cells of a monolayer, with $[Ca^{2+}]$ being higher in the nuclear and perinuclear area; however, hydroxyurea treatment and serum deprivation had no influence on the average $[Ca^{2+}]_i$, compared with the monolayers in the exponential growth phase.

Propidium iodide staining of the nucleus is a classical sign of membrane damage and cell death, but propidium iodide-stained cells did not contain enough fura-2 to allow estimation of their $[Ca^{2+}]$. Therefore, only viable, propidium iodide-negative cells were examined. Twenty-four hours after exposure to DCVC, the average $[Ca^{2+}]_i$ increased. In most cells the mitochondria contained lower $[Ca^{2+}]$ than the rest of the cell. Mitochondria with diminished capacity to sequester cytosolic Ca^{2+} could still be stained with rhodamine-123, indicating that the mitochondrial Ca^{2+} release was not associated with a collapse of the mitochondrial membrane potential resulting in a reversal of the Ca^{2+} uniport; selective staining of mitochondria by rhodamine-123 is dependent on the high negative electrical potential across the mitochondrial membrane (28). Ca^{2+} efflux at high mitochondrial membrane potentials may occur via a $Ca^{2+}/2\ H^+$ antiport and is promoted by oxidation and hydrolysis of pyridine nucleotides, followed by a covalent modification of a protein in the liver mitochondrial membrane by mono-(ADP)ribose (29); the effluxed Ca^{2+} may be subsequently taken up by the mitochondrial uniport. This Ca^{2+} cycling imposes a continuous energy drain on mitochondria, which eventually leads to damage that is accompanied by decreased mitochondrial membrane potential and decreased rhodamine-123 uptake by mitochondria. This lack of rhodamine-123 staining was observed after 72- and 96-hr exposure to DCVC (see below). The FDIM observations described above confirm previous biochemical data obtained with DCVC and *S*-(pentachlorobutadienyl)-L-cysteine, the cysteine conjugate of the nephrocarcinogen hexachlorobutadiene. *S*-(Pentachlorobutadienyl)-L-cysteine depletes Ca^{2+} from rat kidney cortical mitochondria (30); in isolated rat kidney cells, DCVC-induced release of mitochondrial Ca^{2+} is associated with inhibition of cellular respiration (31). In spite of the marked changes in the spatial distribution of intracellular Ca^{2+}, few blebs were observed 24 and 48 hr after treatment with DCVC, indicating that Ca^{2+} redistribution and increase of $[Ca^{2+}]_i$ precede the disruption of the cytoskeleton under these conditions.

Previous reports on the mitochondrial toxicity of DCVC and DCVHC in freshly isolated proximal tubule cells failed to reveal marked differences (31). The present studies with FDIM, however, revealed major differences between the effects of DCVC and DCVHC on Ca^{2+} homeostasis. Twenty-four hours after exposure to either DCVC or DCVHC, similar increases in the average $[Ca^{2+}]_i$ were observed; in contrast, DCVHC caused a completely different pattern in the spatial distribution of Ca^{2+} after 24 hr, resulting in higher mitochondrial $[Ca^{2+}]$ compared with the rest of the cell, thus indicating that the mitochondria were still able to sequester cytosolic Ca^{2+}. The differences between LLC-PK$_1$ cells and freshly isolated kidney cells may be due both to the utilization of two different cell types and to the very high sensitivity of the FDIM for determination of microenvironmental redistributions of Ca^{2+}. Moreover, DCVHC inhibits microsomal Ca^{2+} sequestration, whereas DCVC exclusively impairs mitochondrial Ca^{2+} homeostasis (31). Therefore, DCVC may produce more profound impairment of mitochondrial Ca^{2+} sequestration.

On the third and fourth day of exposure to *S*-conjugates, blebs with higher $[Ca^{2+}]$, compared with the rest of the cell, were observed in both DCVC- and DCVHC-treated monolayers, but quantitative differences between the two compounds were observed. Large blebs were found in most cells treated with DCVHC for 3–4 days, whereas some DCVC-treated cells showed a diffuse spatial distribution of elevated $[Ca^{2+}]$ without blebs. Blebs were observed in cells that did not take up propidium iodide, which is consistent with previous reports showing that blebbing of the cell surface occurs before changes in membrane permeability can be detected (32, 33). In addition, although the mitochondria of the DCVHC-treated cells could be stained with rhodamine-123 after 96-hr exposure, this was not the case with DCVC, indicating that DCVC causes severe mitochondrial damage, including the loss of mitochondrial membrane potential (31).

Bleb formation is associated with sustained high elevations of $[Ca^{2+}]_i$ (9, 34, 35), although this has been contested (36). The observations described herein show that elevated $[Ca^{2+}]_i$ and the marked intracellular redistribution of Ca^{2+} precede bleb formation in *S*-conjugate-damaged LLC-PK$_1$ cells but do

not establish a causal relationship between $[Ca^{2+}]_i$ and bleb formation.

There are two major findings in the present study on the cytotoxicity of *S*-conjugates that have major implications for the biological effects of such compounds. First, redistribution of mitochondrial Ca^{2+} precedes bleb formation and cell death. This is in agreement with the previous observation that mitochondria are major intracellular targets for cysteine *S*-conjugates; mitochondrial damage decreases the ability of mitochondria to retain calcium. Second, DCVC, which promotes *N*,*N*-dimethylnitrosamine-initiated renal tumors (11), induces loss of mitochondrial Ca^{2+} that precedes the collapse of the mitochondrial membrane potential, an effect common to some tumor promoters, such as organic hydroperoxides,that induce oxidative stress and diminished mitochondrial NAD(P)H concentrations (37, 38). Similar effects have been observed with benzoquinone, which impairs the $NAD(P)^+$-reducing capacity of isolated rat liver mitochondria by arylation of critical thiol groups of NAD(P)H dehydrogenases (39), and DCVC also inhibits sulfhydryl-sensitive dehydrogenases in isolated rat liver and kidney mitochondria (3). Ca^{2+} release from mitochondria before severe disturbances of their membrane potential is associated with oxidation and hydrolysis of mitochondrial pyridine nucleotides and ADP-ribosylation of mitochondrial membrane proteins. Energy-consuming Ca^{2+} release and reuptake via the Ca^{2+} antiport and uniport result in loss of the mitochondrial membrane potential. These observations confirm and extend previous studies demonstrating that mitochondria are primary cellular targets for cytotoxic *S*-conjugates (3, 30). Further studies to establish the molecular mechanism and the role of *S*-conjugate-induced mitochondrial Ca^{2+} movements as a link between acute cell injury and long term processes contributing to the production of renal tumors are warranted.

References

1. Dekant, W., S. Vamvakas, and M. W. Anders. Bioactivation of nephrotoxic haloalkenes by glutathione conjugation: formation of toxic and mutagenic intermediates by cysteine conjugate β-lyase. *Drug Metab. Rev.* **20**:43–83 (1989).
2. Jaffe, D. R., A. J. Gandolfi, and R. B. Nagle. Chronic toxicity of *S*-(*trans*-1,2-dichlorovinyl)-L-cysteine in mice. *J. Appl. Toxicol.* **4**:315–319 (1984).
3. Lash, L. H., and M. W. Anders. Mechanism of *S*-(1,2-dichlorovinyl)-L-cysteine and *S*-(1,2-dichlorovinyl)-L-homocysteine-induced renal mitochondrial toxicity. *Mol. Pharmacol.* **32**:549–556 (1987).
4. Stevens, J., P. Hayden, and G. Taylor. The role of glutathione conjugate metabolism and cysteine conjugate β-lyase in the mechanism of *S*-cysteine conjugate toxicity in LLC-PK_1 cells. *J. Biol. Chem.* **261**:3325–3332 (1986).
5. Green, T., and J. Odum. Structure/activity studies on the nephrotoxic and mutagenic action of cysteine conjugates of chloro- and fluoroalkenes. *Chem. Biol. Interact.* **54**:15–31 (1985).
6. Dekant, W., S. Vamvakas, K. Berthold, S. Schmidt, D. Wild, and D. Henschler. Bacterial β-lyase mediated cleavage and mutagenicity of cysteine conjugates derived from the nephrocarcinogenic alkenes trichloroethylene, tetrachloroethylene and hexachlorobutadiene. *Chem. Biol. Interact.* **60**:31–45 (1986).
7. Vamvakas, S., W. Dekant, and D. Henschler. Assessment of unscheduled DNA synthesis in a cultured line of renal epithelial cells exposed to cysteine *S*-conjugates of haloalkenes and haloalkanes. *Mutat. Res.* **222**:329–335 (1989).
8. Jaffe, D. R., D. Hassall, J. A. Gandolfi, and K. Brendel. Production of DNA single strand breaks in rabbit renal tissue after exposure to 1,2-dichlorovinylcysteine. *Toxicology* **35**:25–33 (1985).
9. Phelps, P. C., M. W. Smith, and B. F. Trump. Cytosolic ionized calcium and bleb formation after acute cell injury of cultured rabbit renal tubule cells. *Lab. Invest.* **60**:630–642 (1989).
10. Orrenius, S., D. J. McCouley, G. Bellomo, and P. Nicotera. Role of Ca^{2+} in toxic cell killing. *Trends Pharmacol. Sci.* **10**:281–285 (1989).
11. Meadows, S. D., A. J. Gandolfi, R. B. Nagle, and J. W. Shively. Enhancement of DMN-induced kidney tumors by 1,2-dichlorovinyl-cysteine in Swiss-Webster mice. *Drug Chem. Toxicol.* **11**:307–318 (1988).
12. Anderson, P. M., and M. O. Schultz. Cleavage of *S*-(1,2-dichlorovinyl)-L-cysteine by an enzyme of bovine origin. *Arch. Biochem. Biophys.* **111**:593–602 (1965).
13. McKinney, L. L., J. C. Picken, F. B. Weakley, A. C. Eldridge, R. E. Campbell, J. C. Cowan, and H. E. Biester. Possible toxic factor of trichloroethylene-extracted soybean oil meal. *J. Am. Chem. Soc.* **81**:909–915 (1959).
14. Elfarra, A. A., I. Jakobson, and M. W. Anders. Metabolic activation and detoxication of nephrotoxic cysteine and homocysteine *S*-conjugates. *Proc. Natl. Acad. Sci. USA* **83**:2667–2671 (1986).
15. Poenie, M., J. Alderton, R. Steinhardt, and R. Tsien. Calcium rises abruptly and briefly throughout the cell at the onset of anaphase. *Science (Washington D. C.)* **233**: 886–889 (1986).
16. Williford, D. J., M. K. Walton, and S.-S. Sheu. Fluorescence digital imaging microscopy: spatial distribution of Ca^{2+} and H^+ in single cells, in *Microcompartmentation* (D. P. Jones, ed.). CRC Press, Inc., Boca Raton, FL, 228–249 (1989).
17. Williford, D. J., V. K. Sharma, M. Korth, and S.-S. Sheu. Spatial heterogeneity of intracellular Ca^{2+} concentration in nonbeating guinea pig ventricular myocytes. *Circ. Res.* **66**:234–241 (1990).
18. Fabiato, A. Computer programs for calculating total from specified free or free from specified total ionic concentrations in aqueous solutions containing multiple metals and ligands. *Methods Enzymol.* **157**:378–417 (1988).
19. Grynkiewicz, G., M. Poenie, and R. Y. Tsien. A new generation of Ca^{2+} indicators with greatly improved fluorescence properties. *J. Biol. Chem.* **260**:3440–3450 (1985).
20. Vamvakas, S., W. Dekant, D. Schiffmann, and D. Henschler. Characterization of an unscheduled DNA synthesis assay with a cultured line of porcine kidney cells (LLC-PK_1), in *Nephrotoxicity: Extrapolation from In Vitro to In Vivo and from Animals to Man* (P. H. Bach and E. A. Lock, eds.). Plenum Press, New York, 749–755 (1989).
21. Malgaroli, A., D. Milani, J. Meldolesi, and T. Pozzan. Fura-2 measurement of cytosolic free Ca^{2+} in monolayers and suspensions of various types of animal cells. *J. Cell Biol.* **105**:2145–2155 (1987).
22. Di Virgilio, F., T. H. Steinberg, J. A. Swanson, and S. C. Silverstein. Fura-2 secretion and sequestration in macrophages. *J. Immunol.* **140**:915–920 (1988).
23. Scanlon, M., D. A. Williams, and S. F. Fay. A Ca^{2+}-insensitive form of fura-2 associated with polymorphonuclear leucocytes: assessment and accurate Ca^{2+} measurement. *J. Biol. Chem.* **262**:6308–6312 (1987).
24. Ratan, R. R., M. Shelanski, and F. R. Maxfield. Transition from metaphase to anaphase is accompanied by local changes in cytoplasmic free Ca^{2+} in PTK2 kidney epithelial cells. *Proc. Natl. Acad. Sci. USA* **83**:5136–5140 (1986).
25. Holohan, P. D., P. P. Sokol, C. R. Ross, R. Coulson, M. E. Trimble, D. A. Laska, and P. D. Williams. Gentamicin-induced increases in cytosolic calcium in pig kidney cells (LLC-PK_1). *J. Pharmacol. Exp. Ther.* **247**:349–354 (1988).
26. Inui, K.-I., H. Saito, T. Iwata, and R. Hori. Aminoglycoside-induced alterations in apical membranes of kidney epithelial cell line (LLC-PK_1). *Am. J. Physiol.* **254**:C251–C257 (1988).
27. Stassen, F. L., G. Heckman, D. Schmidt, M. T. Papadopoulos, P. Nambi, H. Sarau, N. Aiyar, M. Gellai, and L. Kinter. Oxytocin induces a transient increase in cytosolic free $[Ca^{2+}]$ in renal tubular epithelial cells: evidence for oxytocin receptors in LLC-PK_1 cells. *Mol. Pharmacol.* **33**:218–224 (1988).
28. Johnson, L. V., M. L. Walsh, and L. B. Chen. Localization of mitochondria in living cells with rhodamine 123. *Proc. Natl. Acad. Sci. USA* **77**:990–994 (1980).
29. Richter, C, and F. Balz. Ca^{2+} movements induced by hydroperoxides in mitochondria, in *Oxidative Stress* (H. Sies, ed.). Academic Press Inc., London, 221–241 (1985).
30. Wallin, A., T. W. Jones, A. E. Vercesi, I. Cotgreave, K. Ormstad, and S. Orrenius. Toxicity of *S*-pentachlorobutadienyl-L-cysteine studied with isolated rat renal cortical mitochondria. *Arch. Biochem. Biophys.* **258**:365–372 (1987).
31. Lash, L. H., A. A. Elfarra, and M. W. Anders. *S*-(1,2-Dichlorovinyl)-L-homocysteine-induced cytotoxicity in isolated rat kidney cells. *Arch. Biochem. Biophys.* **251**:432–439 (1986).
32. Jewell, S. A., G. Bellomo, H. Thor, and S. Orrenius. Bleb formation in hepatocytes during drug metabolism is caused by disturbances in thiol and calcium ion homeostasis. *Science (Washington D. C.)* **217**:1251–1259 (1982).
33. Boobis, A. R., J. Fawtheron, and D. S. Davis. Mechanisms of cell death. *Trends Pharmacol. Sci.* **10**:275–280 (1989).
34. Nicotera, P., P. Hartell, G. Davis, and S. Orrenius. The formation of plasma membrane blebs in hepatocytes exposed to agents that increase cytosolic Ca^{2+} is mediated by the activation of a non-lysosomal proteolytic system. *FEBS Lett.* **209**:139–144 (1986).
35. Richelmi, P., F. Mirabelli, A. Salis, G. Finardi, F. Berte, and G. Bellomo. On the role of mitochondria in cell injury caused by vanadate-induced Ca^{2+} overload. *Toxicology* **57**:29–44 (1989).
36. Lemasters, J. J., J. DiGuiseppi, A.-L. Nieminen, and B. Herman. Blebbing, free Ca^{2+} and mitochondrial membrane potential preceding cell death in hepatocytes. *Nature (Lond.)* **325**:78–81 (1987).
37. Trump, B. F. and I. K. Berezesky. Ion regulation, cell injury and carcinogenesis. *Carcinogenesis (Lond.)* **8**:1027–1030 (1987).
38. Cerutti, P. A. Prooxidant states and tumor promotion. *Science (Washington D. C.)* **227**:375–381
39. Moore, G. A., M. Weis, S. Orrenius, and P. J. O'Brien. Role of sulfhydryl groups in benzoquinone-induced Ca^{2+} release by rat liver mitochondria. *Arch. Biochem. Biophys.* **267**:539–550 (1988).

Send reprint requests to: M. W. Anders, Department of Pharmacology, University of Rochester, 601 Elmwood Avenue, Rochester, NY 14642.